

# High-sensitivity strain sensor based on inflated long period fiber grating

Xiaoyong Zhong,<sup>1</sup> Yiping Wang,<sup>1,2</sup> Junle Qu,<sup>1,3</sup> Changrui Liao,<sup>1</sup> Shen Liu,<sup>1</sup> Jian Tang,<sup>1</sup> Qiao Wang,<sup>1</sup> Jing Zhao,<sup>1</sup> Kaiming Yang,<sup>1</sup> and Zhengyong Li<sup>1</sup>

<sup>1</sup>Key Laboratory of Optoelectronic Devices and Systems of Ministry of Education and Guangdong Province, College of Optoelectronic Engineering, Shenzhen University, Shenzhen 518060, China

<sup>2</sup>e-mail: ypwang@szu.edu.cn

<sup>3</sup>e-mail: jlqu@szu.edu.cn

Received July 11, 2014; revised August 17, 2014; accepted August 18, 2014;  
posted August 19, 2014 (Doc. ID 216723); published September 15, 2014

We demonstrated a high-sensitivity strain sensor based on an inflated long period fiber grating (I-LPFG). The I-LPFG was inscribed, for the first time to the best of our knowledge, by use of the pressure-assisted CO<sub>2</sub> laser beam scanning technique to inflate periodically air holes of a photonic crystal fiber. Such periodic inflations enhanced the sensitivity of the LPFG-based strain sensor to  $-5.62 \text{ pm}/\mu\epsilon$ . After high temperature annealing, the I-LPFG achieved a good repeatability and stability of temperature response with a sensitivity of  $11.92 \text{ pm}/^\circ\text{C}$ . © 2014 Optical Society of America

OCIS codes: (060.5295) Photonic crystal fibers; (050.2770) Gratings; (060.2340) Fiber optics components; (060.2370) Fiber optics sensors.

<http://dx.doi.org/10.1364/OL.39.005463>

Long period fiber gratings (LPFGs) inscribed in photonic crystal fibers (PCFs) have been extensively explored for telecommunication and sensor applications [1–3]. Various inscription methods, such as CO<sub>2</sub> laser irradiation [4,5], electric arc discharge [6,7], mechanical pressure [8,9], and femtosecond laser exposure [10,11], have been demonstrated to write LPFGs in different types of PCFs. Among these methods, the CO<sub>2</sub> laser irradiation method is particularly flexible and low cost, because it could be applied to write a LPFG in a pure-silica PCF without photosensitivity [12,13] and a hollow-core photonic bandgap fiber (PBF) [14]. And the writing process usually is computer programmed to produce complicated grating profiles. Unfortunately, the strain sensitivity of the CO<sub>2</sub>-laser-induced LPFGs without physical deformation is usually very low, e.g., only  $-0.45 \text{ pm}/\mu\epsilon$  and  $-0.19 \text{ pm}/\mu\epsilon$  in Corning SMF-28 fiber [15] and in the PCF [12], respectively. Recently a pressure-assisted electrode arc discharge (EAD) technique was first demonstrated to avoid the collapse of air holes during the inscription of a LPFG in a hollow-core PBF [16].

In this Letter, a type of novel inflated long period fiber gratings (I-LPFGs) was inscribed in a solid-core PCF by use of a pressure-assisted CO<sub>2</sub> laser beam scanning technique to inflate periodically air holes along the fiber axis. To the best of our knowledge, the I-LPFG was inscribed successfully in a solid-core PCF for the first time. Such an I-LPFG exhibited a high strain sensitivity of  $-5.62 \text{ pm}/\mu\epsilon$  attributable to periodic inflations of air holes.

We built a CO<sub>2</sub> laser irradiation system for inscribing an I-LPFG in a PCF by means of improving the experimental setup reported in Ref. [17] and integrating a high-pressure air pump. As shown in Fig. 1, such a system consisted of an industrial CO<sub>2</sub> laser with a maximum power of 10 W (SYNRAD 48-1) and a power stability of  $\pm 2\%$ , an electric shutter for turning on/off the laser beam, an infrared lens with a focused length of 63.5 mm, a four-times beam expander for decreasing the diameter of the focused laser spot, and a computer-controlled

two-dimensional ultra-precision translation stage with a minimum incremental motion of 10 nm and a bi-directional repeatability of 80 nm. A PCF (NKT LMA-10) was employed and situated at the focal plane of the CO<sub>2</sub> laser beam and then periodically exposed via the computer-controlled two-dimensional translation stage. A broadband light source (NKT Photonics SuperK) and an optical spectrum analyzer (OSA) (YOKOGAWA AQ6370C) were employed to monitor transmission spectrum evolution of the inscribed LPFG. An air pump with a maximum pressure of 2.5 MPa was employed to provide high-pressure air inside the holes of the PCF, as described below.

First, as shown in Fig. 1(b), an end of a silica tube with an inner/outer diameter of 75/127  $\mu\text{m}$  was spliced with a single-mode fiber (SMF) by use of a commercial fusion

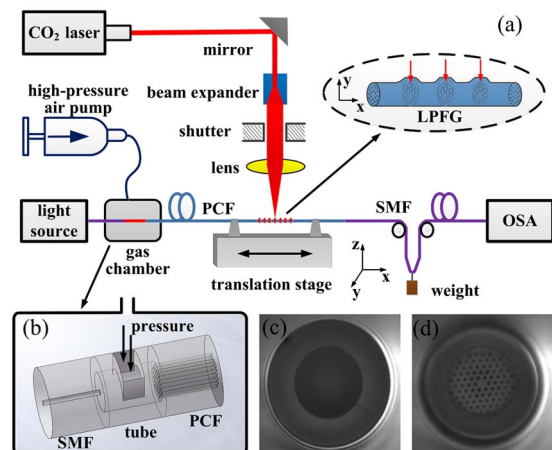


Fig. 1. (a) Experimental setup for I-LPFG inscription with a pressure-assisted CO<sub>2</sub> laser beam scanning technique, (b) schematic diagram of the gas chamber for air passing through the silica tube into air holes of the PCF, (c) and (d) microscope images of the cross sections of the silica tube and the PCF located at the spliced joint.

splicer (FSM-60) in the manual mode. Second, another end of the silica tube was cleaved to shorten its length to be  $\sim 100\ \mu\text{m}$  and then spliced with a PCF (NKT LMA-10). As shown in Fig. 1(d), although air holes located within the two outer rings were sealed due to arc discharge, the rest of the air holes of the PCF at the spliced joint between the silica tube and the PCF were still open so that air could pass through the silica tube into the holes of the PCF. Third, a microcavity ( $50 \times 40\ \mu\text{m}$ ) was fabricated on the sidewall of the silica tube by use of a femtosecond laser pulse (with a central wavelength of 800 nm, a pulse duration time of 120 fs, and a repetition rate of 1 kHz) to create a channel so that air could pass from the gas chamber into the silica tube. Fourth, another end of the PCF was spliced with another SMF and then attached with a small weight of  $\sim 5\ \text{g}$  to keep the fiber straight and to provide a constant prestrain in the fiber, thus enhancing the efficiency of grating inscription [18]. Finally, the silica tube with a channel was placed into a gas chamber, as illustrated in Fig. 1(b).

As shown in Figs. 1 and 2(a), air with a pressure of 1.5 MPa accessed the holes of the PCF via the gas chamber by use of the high-pressure air pump. As shown in Fig. 2(b), the PCF was periodically heated along the fiber axis by the focused  $\text{CO}_2$  laser beam. As shown in Fig. 2(c), the holes of the PCF were inflated within the heated region, resulting from high-pressure air and the  $\text{CO}_2$ -laser-induced high temperature. Such inflations induce periodically refractive index modulation along the fiber axis, thus inscribing an I-LPFG in the PCF. The periodical heating process above may be repeated for  $K$  cycles from the first grating period to the last grating period until a desired I-LPFG is achieved. As shown in Fig. 3, a high-quality I-LPFG with 30 grating periods and a grating pitch of  $480\ \mu\text{m}$  was inscribed in the PCF after the number of scanning cycles ( $K$ ) increased from 1 to 11, where the attenuations at the resonant wavelengths of Dip<sub>1</sub> and Dip<sub>2</sub> are  $-30.2\ \text{dB}$  at  $1581.4\ \text{nm}$  and  $-5.5\ \text{dB}$  at  $1441.1\ \text{nm}$ , respectively.

During grating inscription, it is very necessary to real-time monitor the transmission spectrum evolution for achieving a desired LPFG with a required resonant

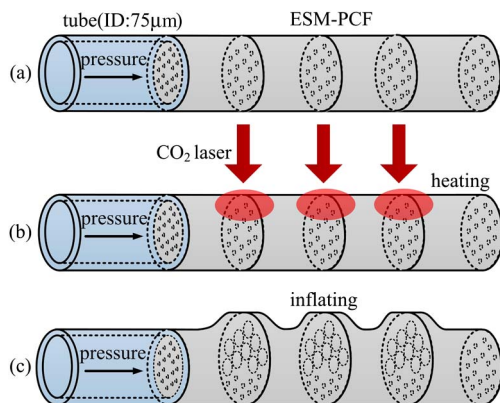


Fig. 2. Schematic diagram of I-LPFG inscription in a PCF with  $\text{CO}_2$  laser irradiation. (a) High-pressure air accessed into the holes of the PCF via the gas chamber. (b) The PCF was periodically heated along the fiber axis by the focused  $\text{CO}_2$  laser beam. (c) The holes of the PCF were periodically inflated along the fiber axis, and thus inscribing an I-LPFG in the PCF.

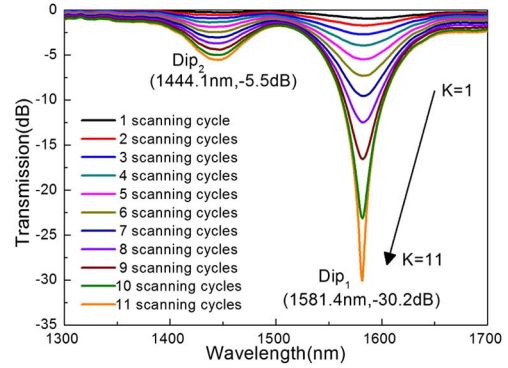


Fig. 3. Transmission spectrum evolution of a  $\text{CO}_2$ -laser-inscribed I-LPFG with 30 grating periods and a grating pitch of  $480\ \mu\text{m}$  while the number of scanning cycles ( $K$ ) increases from 1 to 11.

wavelength and attenuation dip. In case air was directly pumped into air holes of the PBF end, as reported in [16], it is impossible to real-time monitor the transmission spectrum evolution during grating inscription. So an improved pressure-assisted technique was demonstrated in our experiments, as shown in Fig. 1. That is, the silica tube with a created channel was spliced with the PCF end in order to monitor in real-time the transmission spectrum evolution of the I-LPFG during grating inscription. We inscribed a few I-LPFGs with the same grating pitch and number of grating periods, and the results exhibit an excellent repeatability with a small wavelength error of less than  $\pm 5\ \text{nm}$ , which indicates a good, consistent result for grating inscription.

As shown in Fig. 4(a), air holes of the PCF employed have an average diameter of  $1.8\ \mu\text{m}$  and a center-to-center distance of  $6.1\ \mu\text{m}$ . The core and cladding diameters of the PCF are  $10.4$  and  $125\ \mu\text{m}$ , respectively. We observed the cross sections of the PCF by use of a microscope before and after  $\text{CO}_2$  laser irradiation. As shown in Figs. 4(b) and 4(c), part of the air holes clearly inflated within the fiber side facing the  $\text{CO}_2$  laser irradiation, which resulted from the single-side irradiation of the  $\text{CO}_2$  laser and the strong  $\text{CO}_2$  laser energy absorption of silica glass. Compared with the PCF diameter of  $125\ \mu\text{m}$ , the inflated region of the PCF has a diameter of  $130\ \mu\text{m}$  along the  $\text{CO}_2$  laser irradiation direction.

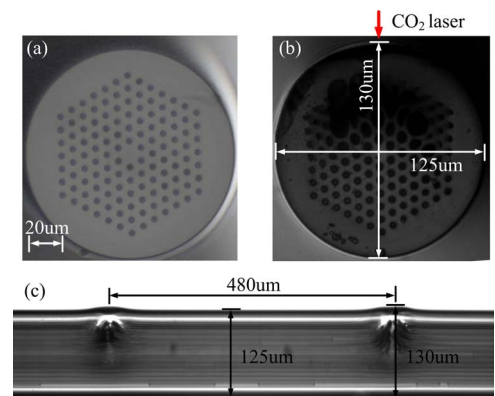


Fig. 4. Microscope image of the cross section of the PCF (a) before and (b) after  $\text{CO}_2$  laser irradiation, (c) side view of the  $\text{CO}_2$ -laser-inscribed I-LPFG with periodic inflation.

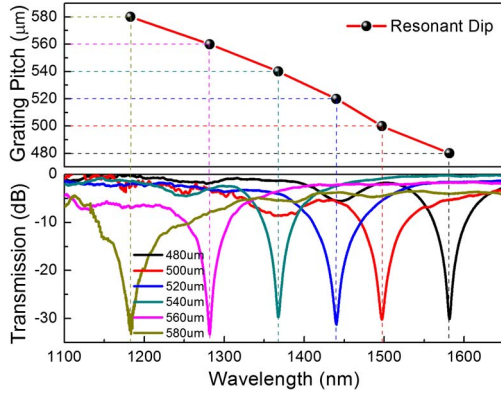


Fig. 5. Variation of I-LPFG resonant wavelengths with grating pitch (upper panel) and their transmission spectra (lower panel). These I-LPFGs are with 30 grating periods and grating pitches of 480, 500, ..., and 580  $\mu\text{m}$ , respectively.

Uneven expansion of the holes illustrated in Fig. 4(b) may be due to the inhomogeneity of the holes in the PCF. So the I-LPFG is an asymmetrical in-fiber grating, thus resulting in a high strain sensitivity [13,19], as described below.

To investigate the phase matching condition as a function of resonant wavelength, six I-LPFGs with the same number of grating periods ( $N = 30$ ) and different pitches of 480, 500, ..., and 580  $\mu\text{m}$  were inscribed in the PCF. We measured their transmission spectra and resonant wavelengths as functions of the grating pitch. As shown in Fig. 5, the resonant wavelength of the I-LPFGs decreases with the increase of grating pitch, which is opposite to the LPFGs in the conventional SMFs, and in agreement with the previously reported results of LPFGs inscribed in solid-core PCFs [11,20] and in air-core photonic bandgap fibers [14].

A polarization controller was integrated between the light source and the inscribed I-LPFG to investigate the influence of the grating birefringence. While the fiber loops of the polarization controller were rotated to change the state of polarization of the input light, as shown in Fig. 6, the attenuation dip of the I-LPFG was split into two dips corresponding to two polarized light resonance, which indicates that the I-LPFG has a high birefringence due to asymmetric inflations resulting from single-side  $\text{CO}_2$  laser exposure. Detailed birefringence

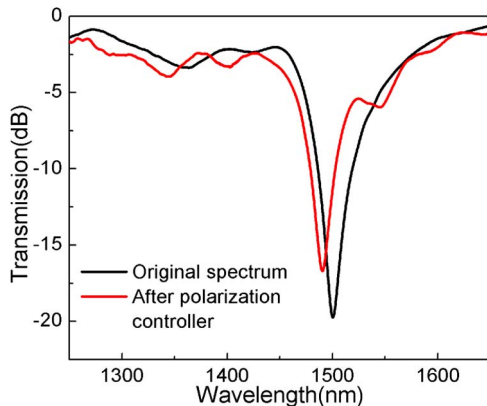


Fig. 6. Transmission spectra of the I-LPFG with (red curve) and without (black curve) using a polarization controller.

response and polarization dependent loss of the I-LPFG will be investigated in our further work.

We investigated the strain responses of the I-LPFG sample with a pitch of 480  $\mu\text{m}$ . The resonant wavelength of the I-LPFG was measured while the tensile strain was increased from 0 to 500  $\mu\epsilon$  with a step of 50  $\mu\epsilon$ . An OSA and a light source were employed to monitor transmission spectrum evolution of the I-LPFG during stretching the grating sample. As shown in Fig. 7(a), the resonant wavelength was shifted linearly toward a shorter wavelength with the increased tensile strain. As shown in Fig. 7(b), the strain sensitivity of the I-LPFG is  $-5.62 \text{ pm}/\mu\epsilon$ , which is one order of magnitude higher than that of the conventional  $\text{CO}_2$ -laser-induced LPFGs written in the same type of PCF in which no air holes were periodically inflated [12]. In contrast, the peak transmission attenuation of I-LPFG is hardly changed with an increase of the tensile strain. It is obvious that periodic inflations in our I-LPFGs enhance effectively the strain sensitivity of the grating. The reason for this could be the asymmetry of the I-LPFG and the stretch-induced periodic microbends along the fiber axis [13,19]. Another five I-LPFG samples with different grating pitches illustrated in Fig. 5 were also investigated; and similar strain sensitivity were achieved. Here, only the strain response of the grating sample with a pitch of 480  $\mu\text{m}$  was given in Fig. 7. So our I-LPFGs could be used to develop high-sensitivity strain sensors.

We investigated the annealing behavior of our I-LPFGs to improve the repeatability of their temperature

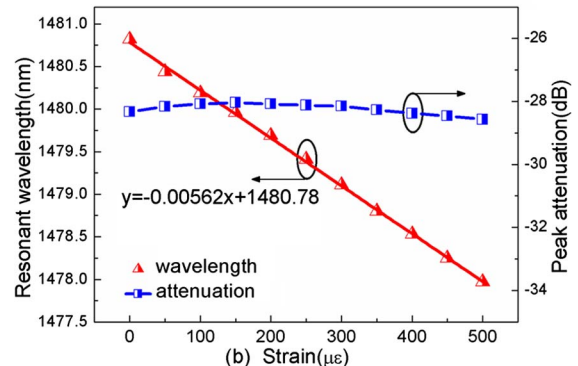
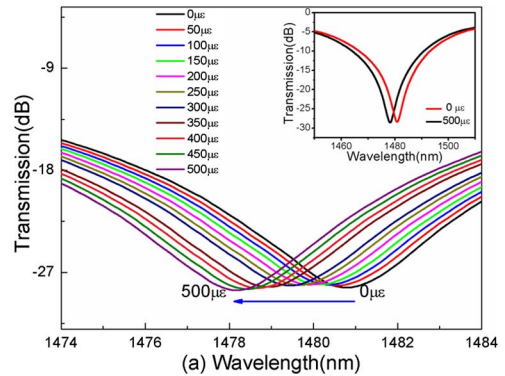


Fig. 7. (a) Transmission spectrum evolution of an I-LPFG sample with a pitch of 480  $\mu\text{m}$  while the tensile strain increases from 0 to 500  $\mu\epsilon$ . Inset illustrates the transmission spectrum evolution within a large wavelength range. (b) Measured resonant wavelength and peak attenuation of the I-LPFG as a function of tensile strain.

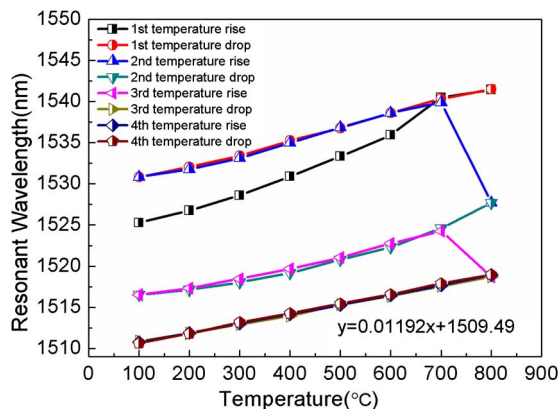


Fig. 8. Measured resonant wavelength of the I-LPFG during temperature rising and dropping.

response. An I-LPFG with a period of 480  $\mu\text{m}$  was placed in a tube furnace whose temperature can rise from room temperature to 800°C. An OSA and a light source were employed to monitor transmission spectrum evolution of the I-LPFG during heating and cooling the grating sample. The I-LPFG sample was heated from 100°C to 800°C with a step of 100°C, and then cooled down to 100°C in the same step. After a desired temperature was achieved each time, the temperature was maintained for 30 min, and then the resonant wavelength of the I-LPFG was recorded. Such a temperature rise-and-drop cycle was repeated four times to anneal the I-LPFG. During temperature rising or dropping, as shown in Fig. 8, the resonant wavelength shifted toward a longer or shorter wavelength, respectively. The resonant wavelength occurred as a sharp shift at the temperature of about 700°C–800°C at the first, second, and third temperature rise-and-drop cycles, which may result from the glass densification, frozen-in stresses, or glass volume expanding [20,21]. At and after the fourth temperature rise-and-drop cycle, the resonant wavelength linearly shifted with a sensitivity of 11.92 pm/°C, and good repeatability was observed during temperature rising and dropping. So the anneal experiment improved effectively the repeatability of the I-LPFG's temperature response. Other I-LPFG samples with different grating pitches were also annealed with the same process above, and similar temperature responses were observed. Similar to the temperature response above and reported in [13,22], the LPFGs inscribed in pure-silica PCFs exhibit a low-temperature sensitivity or insensitivity to temperature due to the pure-silica core, which could reduce or avoid the cross sensitivity between strain and temperature in practical sensing applications.

In summary, we demonstrated a novel method for inscribing an I-LPFG in a PCF by using the pressure-assisted CO<sub>2</sub> laser beam scanning technique. This technique combined with pressure actuation inside air holes can modify the size and shape of the holes and thus induce refractive index perturbation of the PCF. The PCF's holes filled with high-pressure air were periodically heated and inflated by use of a focus CO<sub>2</sub> laser

beam, and thus formed an I-LPFG. Periodic inflations of the holes enhanced the strain sensitivity of the I-LPFG to  $-5.62 \text{ pm}/\mu\epsilon$ . Hence, such an I-LPFG could be used to develop a promising high-sensitivity strain sensor. Moreover, after high temperature annealing, the I-LPFG demonstrated a good repeatability and stability of temperature response, and a sensitivity of 11.92 pm/°C was achieved.

This work was supported by the National Science Foundation of China (Grant Nos. 61308027, 61377090, and 11174064), the Science & Technology Innovation Commission of Shenzhen (Grant Nos. KQCX20120815161444632 and JCYJ20130329140017262), and the Distinguished Professors Funding from Shenzhen University and Guangdong Province Pearl River Scholars.

## References

1. Y. Wang, *J. Appl. Phys.* **108**, 081101 (2010).
2. L. Rindorf, J. B. Jensen, M. Dufva, L. H. Pedersen, and O. Bang, *Opt. Express* **14**, 8224 (2006).
3. Y. P. Wang, L. M. Xiao, D. N. Wang, and W. Jin, *Opt. Lett.* **32**, 1035 (2007).
4. G. Kakarantzas, T. Birks, and P. S. J. Russell, *Opt. Lett.* **27**, 1013 (2002).
5. Y. P. Wang, Y. J. Rao, Z. L. Ran, T. Zhu, and A. Z. Hu, *IEEE Photon. Technol. Lett.* **15**, 251 (2003).
6. G. Humbert, A. Malki, S. Fevrier, P. Roy, and D. Pagnoux, *Electron. Lett.* **39**, 349 (2003).
7. H. Y. Choi, K. S. Park, and B. H. Lee, *Opt. Lett.* **33**, 812 (2008).
8. J. H. Lim, K. S. Lee, J. C. Kim, and B. H. Lee, *Opt. Lett.* **29**, 331 (2004).
9. D. Noordegraaf, L. Scolari, J. Lšgsgaard, L. Rindorf, and T. T. Alkeskjold, *Opt. Express* **15**, 7901 (2007).
10. C. Florea and K. A. Winick, *J. Lightwave Technol.* **21**, 246 (2003).
11. S. Liu, L. Jin, W. Jin, D. Wang, C. Liao, and Y. Wang, *Opt. Express* **18**, 5496 (2010).
12. Y. Zhu, P. Shum, H.-W. Bay, M. Yan, X. Yu, J. Hu, J. Hao, and C. Lu, *Opt. Lett.* **30**, 367 (2005).
13. Y. P. Wang, L. M. Xiao, D. N. Wang, and W. Jin, *Opt. Lett.* **31**, 3414 (2006).
14. Y. Wang, W. Jin, J. Ju, H. Xuan, H. L. Ho, L. Xiao, and D. Wang, *Opt. Express* **16**, 2784 (2008).
15. Y. J. Rao, Y. P. Wang, Z. L. Ran, and T. Zhu, *J. Lightwave Technol.* **21**, 1320 (2003).
16. A. Iadicicco, S. Campopiano, and A. Cusano, *IEEE Photon. Technol. Lett.* **23**, 1567 (2011).
17. X. Y. Zhong, Y. P. Wang, C. R. Liao, G. L. Yin, J. T. Zhou, G. J. Wang, B. Sun, and J. Tang, *IEEE Photon. J.* **6**, 2201508 (2014).
18. H. W. Lee and K. S. Chiang, *Opt. Express* **17**, 4533 (2009).
19. Y. P. Wang, D. N. Wang, W. Jin, Y. J. Rao, and G. D. Peng, *Appl. Phys. Lett.* **89**, 151105 (2006).
20. K. Morishita and Y. Miyake, *J. Lightwave Technol.* **22**, 625 (2004).
21. Y. J. Rao, D. W. Duan, Y. E. Fan, T. Ke, and M. Xu, *J. Lightwave Technol.* **28**, 1530 (2010).
22. H. Dobb, K. Kalli, and D. J. Webb, *Electron. Lett.* **40**, 657 (2004).